JOURNAL OF OPTOELECTRONICS AND ADVANCED MATERIALS Vol. 10, No. 7, July 2008, p. 1749 - 1753

Influence of gases on conductivity of onion-like carbon and multiwalled carbon nanotubes

A. I. ROMANENKO[a,b *], O. B. ANIKEEVA[a,b], V. L. KUZNETSOV[b, c], T. I. BURYAKOV[a,b], E. N. TKACHEV[a,b], S. I. MOSEENKOV[b, c], A. N. USOLTSEVA[b, c]
[a]*Nikolaev Institute of Inorganic Chemistry Siberian Branch of Russian Academy of Science, Novosibirsk, Russia*
[b]*Novosibirsk State University, Novosibirsk, Russia*
[c]*Boreskov Institute of Catalysis Siberian Branch of Russian Academy of Science, Novosibirsk, Russia*

Temperature dependences of the conductivity of onion-like carbon (OLC) and catalytic multiwalled carbon nanotubes (MWNTs) were measured in various gas environments: helium, hydrogen, oxygen, air, methane. We have found that in the vicinity of the melting and vaporization temperatures of oxygen and methane the conductivity sharply decreases for MWNTs (by 2−12%) and for OLC (by 4-12%). The observed reversible changes of the conductivity of investigated samples are discussed in the terms of processes of gases adsorption-desorption on the surface of nanotubes and OLC and breakup-recovery of contacts between nanotubes and particles of OLC as a result of melting and vaporization of environment gases.

(Received April 1, 2008; accepted June 30, 2008)

Keywords: Onion-like carbon, Multiwalled carbon nanotube, Conductivity, Gas sensor

1. Introduction

Recently, the influence of gas adsorption on physical properties of carbon nanoparticles has attracted a considerable interest of researchers. Such interest is caused, basically, by two reasons. The first is an aspiration to create the gas nanosensors [1–3], while the other is the problem of accumulation and storage of hydrogen [4, 5]. One of the main factors of the influence of gases on the physical properties is the gas adsorption in space between nanoparticles [6]. The analysis of calorimetric data has shown that the gas adsorption in space between nanotubes gives the main influence on physical properties [6]. Conductivity measurements are one of the most simple and convenient methods of registration of the response of conducting nanoparticles on the external influence; this response can be used to construct a resistive sensor. In this paper we present the results of the influence of gases on the conductivity of onion like carbon and catalytic multiwalled carbon nanotubes.

2. Experimental and samples

Onion-like carbon (OLC) was synthesized by vacuum annealing of nanodiamond particles at 1850 K.[29] The mean diameter of OLC was 3.5 nm, the distance between two neighbouring layers was ~0.35 nm (Fig.1). Curved lines correspond to graphite-like shells with the distance between them equal to 0.34–0.35 nm. Irregularities in the micrograph of the OLC particle are likely caused by holes in the fullerene-like shells or spiral-like structure of the OLC particle. The OLC was combined to agglomerates with typical dimension 50-500 nm. Some of the agglomerates were surrounded by common graphite layers. MWNTs were synthesized by chemical vapor deposition method (CVD-method) via catalytic decomposition of acetylene on the FeCo-catalysts supported on $CaCO_3$ at 950 K [30]. Distinctive

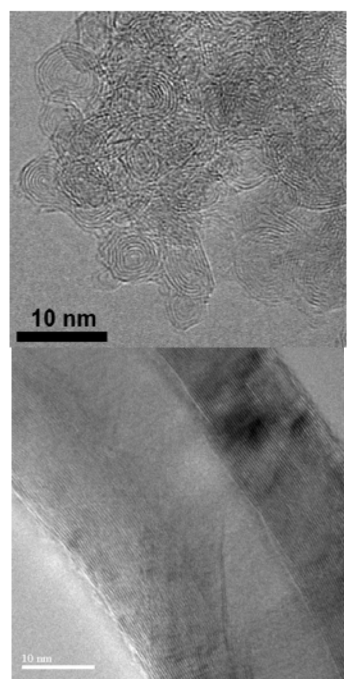

Fig. 1. HRTEM images: top image - OLC particle produced by annealing of ND at 1850 K for 1h in vacuum of 10^{-6} Torr; bottom image – MWNT.

feature of this synthesis is the presence in the reaction environment of oxidizing gas (CO_2), which results from decomposition of $CaCO_3$. The reaction of carbon dioxide with amorphous carbon allows to synthesize pure nanotubes material [7, 8]. After synthesis the MWNTs samples were purified from catalyst by boiling in HCl. The structure of OLC and MWNTs was investigated with using of transmission electron microscopy (TEM) (Fig. 1). According to TEM investigation the synthesized nanotubes material consisted mainly from multiwalled nanotubes with defective structure and didn't contain amorphous carbon. The mean diameter of MWNTs is 20 nm. For electrical measurements the powder of OLC and MWNTs was pressed in a glass ampoule. The electrical contacts were made by 0.1 mm silver wires. The temperature dependences of the conductivity σ(*T*) were measured by four-point-probe technique in the temperature range 4.2–300 K. Our previous researches of powder carbon nanostructures carried out by this method [9–11] showed stability and reproducibility of results of the conductivity measurements.

3 Results and discussion

σ(*T*)/*σ*(300K) *in helium atmosphere*

Before measurements the sample was treated in vacuum (10^{-2} Torr) at 200°C during 12 hours. After that the sample was placed on a measuring platform. We had carried out the degassing of measuring volume in vacuum (10^{-2} Torr) at room temperature during 1 hour and then measuring volume was filled by gaseous helium. According our previous investigations [9-11] for all samples of OLC annealed at temperature higher 1170 K the electrical conductivity showed the temperature dependence typical of the systems with variable range hopping conductivity (VRHC) [12]. For these systems, the temperature dependence of conductivity σ(*T*) may be described by the equation:

$$\sigma(T) = A^{*}\exp[-(T_0/T)^{1/n}] \quad (1)$$

where *A* are constant, the value of *n* is determined by dimensionality *d* of the motion of current carriers as $n=1/(1+d)$ [12], $T_0=C_T\alpha/k_B N(E_F)$, $C_T\sim1$ for one-dimensional VRHC [13, 14], α is the inverse length on which the amplitude of wave function fall down (α~8-10 Å), $N(E_F)$ - density of localized states at the Fermi level, k_B is the Boltzmann constant. Fig. 2 shows the curve of temperature dependence of relative conductivity *σ*(*T*)/*σ*(300K) of OLC (Fig. 2*a*) and MWNTs (Fig. 2*b*). Here *σ*(*T*) - conductivity at temperature *T*, *σ*(300K) - conductivity at room temperature. The data for OLC are described by the Eq. (1) with *n*=2 (one-dimensional VRHC *d*=1) in the all intervals of temperature. The cooling part of *σ*(*T*)/*σ*(300K) curves (in both cases – MWNTs and OLC) coincides with subsequent heating part and any anomalies on the curves are not observed. The temperature dependence of conductivity of MWNTs is described by two-band model [15-16] and at low temperatures (4.2–20 K) is described by the theory of quantum corrections to the conductivity [11, 17-20]. The VRHC (such kind of the dependences as on Fig. 2*a*) or quantum corrections (Fig. 2*b*) is typical for carbon materials with local disorder, for example: OLC [11], catalytic MWNTs [11, 18], arc-produced MWNTs [16], carbon nanocomposites [21, 22], and for graphite-like nanosize crystallites [23]. In order to find out the influence of other gases on conductivity of catalytic MWNTs and OLC we have carried out investigation of *σ*(*T*)/*σ*(300K) behaviour in various gas environments (50% helium and 50% other gas).

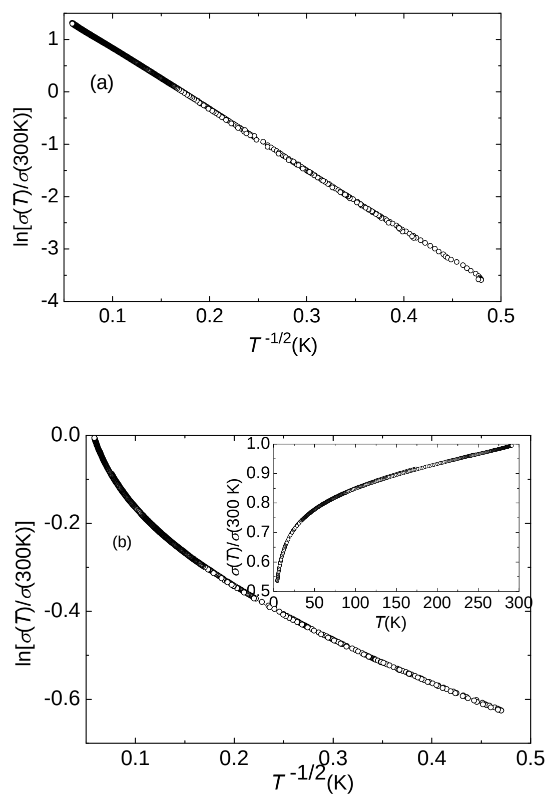

Fig. 2. (a) Relative conductivity in the ln[σ(T)/σ(300K)] - $T^{1/2}$ axis of OLC measured in the helium atmosphere. (b) Relative conductivity in the ln[σ(T)/σ(300K)] - $T^{1/2}$ axis of MWNTs measured in the helium atmosphere. The inset shows relative conductivity of MWNTs in the σ(T)/σ(300K) - T axis.

σ(*T*)/*σ*(300K) *in oxygen-helium atmosphere*

Fig. 3 shows the *σ*(*T*)/*σ*(300K) for OLC (Fig. 3*a*) and for MWNTs (Fig. 3*b*) in the ln[*σ*(*T*)/σ(300K)] - $T^{-1/2}$ axis, which was recorded in the helium-oxygen atmosphere. In

Fig. 3*a* as in the case of Fig. 2*a* the curve is linear in all temperature range in the ln[$\sigma(T)/\sigma$(300K)] – $T^{-1/2}$ axis at cooling process. At heating process the temperature dependence of conductivity is deviated from cooling curve at temperature about 54 K (melting temperature of oxygen) (see inset Fig. 3*a*). At temperature 91-115 K the feature of temperature dependence of conductivity is observed in the ln[$\sigma(T)/\sigma$(300K)] – $T^{-1/2}$ axis. The distinction is obtained between significance of the conductivity on cooling and heating curves at room temperature. In Fig. 3*b* we presented two kinds of curves. The first curve obtained in helium (open circles) is given for comparison. The second curve is received in helium-oxygen atmosphere (filled circles). In the case of helium-oxygen atmosphere the curve of cooling deviates at $T \leq 150$ K from the curve received in helium.

$\sigma(T)/\sigma$(300K) in methane-helium atmosphere

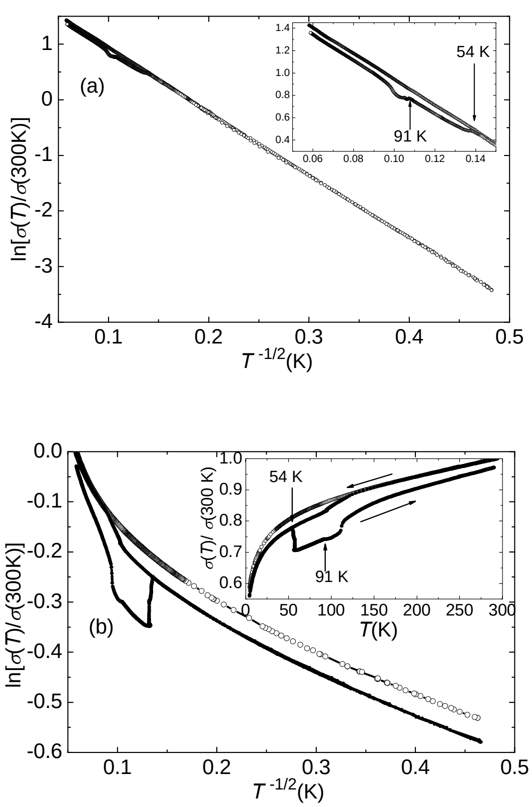

Fig. 3.(a) Relative conductivity in the ln[σ(T)/σ(300K)] – $T^{-1/2}$ axis of OLC measured in the helium-oxygen atmosphere. The inset represents data in the interval from 0.06 – 0.14 $K^{-1/2}$. (b)Relative conductivity in the ln[σ(T)/σ(300K)] – $T^{-1/2}$ axis of MWNTs measured in the helium-oxygen atmosphere (filled circles), the open circles was cited for comparison – curve measured in helium atmosphere. The inset shows the relative conductivity in the σ(T)/σ(300K) - T axis of MWNTs, arrows indicate directions of the temperature change.

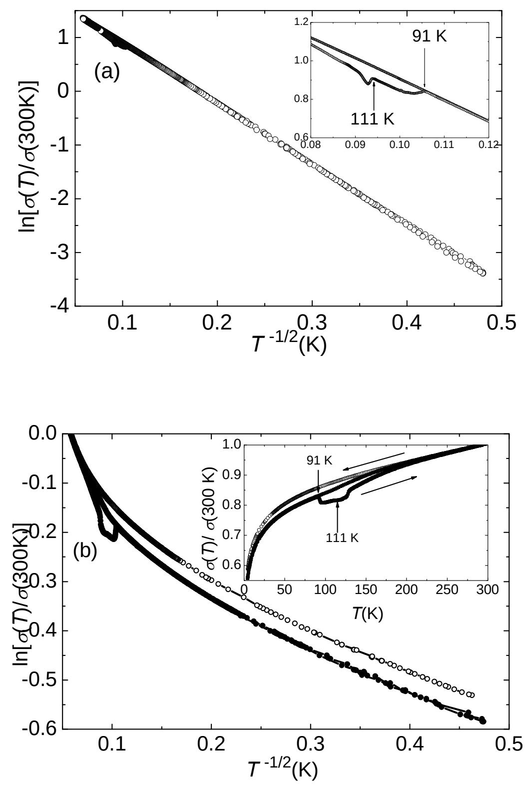

Fig. 4.(a) Relative conductivity in the ln[σ(T)/σ(300K)] – $T^{-1/2}$ axis of OLC measured in the helium-methane atmosphere. The inset represents data in the interval from 0.08 – 0.12 $K^{-1/2}$. (b) Relative conductivity in the ln[σ(T)/σ(300K)] – $T^{-1/2}$ axis of MWNTs measured in the helium-methane atmosphere (filled circles), the open circles cite for comparison – curve measured in helium atmosphere. The inset shows relative conductivity in the σ(T)/σ(300K) - T axis, arrows indicate directions of the temperature change.

Fig. 4 shows the curve $\sigma(T)/\sigma$(300K) for OLC (Fig. 4*a*) and for MWNTs (Fig. 4*b*) in the ln[$\sigma(T)/\sigma$(300K)] – $T^{-1/2}$ axis, which was measured in the helium-methane atmosphere. The cooling curve for OLC (Fig. 4*a*) is linear and similar to curve on Fig. 2*a*. The anomaly is observed on heating curve. The heating curve becomes linear at temperature higher 130 K in the ln[$\sigma(T)/\sigma$(300K)] – $T^{1/2}$ axis. On Fig. 4*b* as well as in a case with oxygen, the curve of cooling deviates from the curve received in helium, but at higher temperature ≈200 K. The curve of heating deviates from the curve of cooling at temperature of methane melting (90.5 K) on the magnitude by ≈5%.

The curves measured in air medium have all anomalies of curves received in oxygen and nitrogen. But the temperatures of these anomalies are 64 and 77 K (air consists of 78% nitrogen) and the magnitude of changes is 4%. The experiments in hydrogen medium are analogous to experiments in air, oxygen and methane mediums, except for magnitude of changes of conductivity (the changes magnitude of conductivity less 1%). Based on the results described above, we suggested a model explaining the behavior of $\sigma(T)$ of MWNTs and OLC in various gases: helium and its mixtures with air, methane, oxygen, and hydrogen. The experimental data indicate that the features of $\sigma(T)$ are related to the presence of a certain gas (except for the inert helium, which produces no features in the temperature interval 4.2-300 K and plays the role of a heat exchange gas).

Kotosonov et al. [15, 16] showed that the electron properties of MWNTs with diameters above 14 nm are analogous to the properties of quasi-two-dimensional (2D) graphite. Using a two-band model of 2D graphite [24, 25], we can propose the following qualitative explanation of the observed temperature dependence of the conductivity of MWNTs. In the ideal MWNTs at T=0, the valence band is completely filled, while the conduction band is partly filled. Owing to the presence of acceptor defects in the carbon layers in real MWNTs, the Fermi level (E_F) is shifted deep in the valence band, which results in the appearance of hole carriers [15]. Since $E_F \sim k_B T$ an increase of the temperature is accompanied by smearing of the Fermi level and significant increase of the carrier density (holes and electrons). This should result in a significant increase of conductivity, which is actually observed in the temperature range from 20 to 300 K (see Fig. 2*b*). In addition to this process the conductivity (see Fig. 3*b*, Fig. 4*b*) changes under the action of adsorbed gases as described in detail below.

When the sample temperature is decreased, the gas adsorbs on the MWNTs surface in the range from a temperature about 200 K to the condensation temperature. This effect is accompanied by a decreasing of the conductivity of MWNTs, because all gases (except for oxygen) physical adsorb on surface and dope nanotubes by electrons [27]. Take into account that the main contribution to the conductivity of MWNTs is related to hole carriers [18, 22], the electron transfer from adsorbed gas molecules to MWNTs leads to a shift of the Fermi level toward to the valence band edge, i.e. to a decreases of the density of holes. This decrease accounts for a decrease of the conductivity, in agreement with our experimental cooling curves. Recently, Jhi et al. [28] demonstrated that oxygen chemisorbed on MWNTs. Take into account that defects in the carbon layers are acceptors [15] we proposed that oxygen leads to modification of these defects, which probably leads to a decrease of the holes density. Consequently, the conductivity decreases in experiments with oxygen (see Fig. 3*b*). At temperatures above the boiling temperature of gas added to helium on heating curve, the conductivity increases owing to desorption of molecules from surface MWNTs in temperature range from T boiling to 200 K (see Fig. 3*b*, Fig. 4*b*).

The velocity of cooling and heating was varied from 60 to 6 K/h, at that the result of experiments is not changed. This implies that the anomalies at melting temperatures of gases (64 K – nitrogen, 54 K – oxygen, 90 K – methane, 14 K – hydrogen) are not connected with prolonged melting of a gas inside nanotubes. At this stage of investigation, we believe that according to the Kelvin equation the cooling leads to capillary condensation of gas primarily at the junctions of nanotubes. After that at the melting temperature on heating curve the condensed gases expand in the solid and then in the liquid phases. This leads to deterioration of the contact between nanotubes and, hence, to a decrease of quantity of charge transport pathways, i.e. the conductivity decreases in the interval between the melting and boiling temperatures of gas. The observed phenomenon consists of two contributions. The first contribution is connected with an irreversible destruction of contacts between individual nanotubes or nanoonions during vaporization of gas and with an increase of the local pressure in the space between two objects. Thus, deformation of nanotubes and onions is occurred. Some nanoobjects are moved and a part of electric contacts between them are irreversible destroyed. The second contribution is connected to an reversible elastic deformation of nanotubes and nanoonions. Reversibility of this deformation is determined by the fact that during heating the hydrogen, oxygen, air and methane vaporizes and quits from nanopores located in sample, the local pressure decreases and the contacts between nanotubes are restored. In the first cooling–heating cycle, as in case of oxygen at room temperature is obtained distinction between significance of conductivity at room temperature on cooling and heating curves because of irreversible deterioration of contacts between MWNTs or due to the residual oxygen adsorbed on the surface of nanotubes and nanoonions. In subsequent cycles, the significance of conductivity returns to the initial level after heating-cooling cycle.

In the case of the OLC in different gases we obtain the result analogous to the MWNTs (Fig. 3*a*, Fig. 4*a*). In all cooling curves the linear dependence in the $\ln[\sigma(T)/\sigma(300\text{K})] - T^{-1/2}$ axis is present. This fact indicate that in OLC adsorbtion and desorption processes are absent. In addition to on heating curves the capillary condensation on OLC is present in all experiments with different gases (except for helium) and the temperatures are coincide with typical boiling and melting temperatures of gases.

4. Conclusion

In summary, we have observed that the variation of gas environment under nanocarbon sample (MWNTs, OLC) leads to significant changes of the conductivity of catalytic multiwalled carbon nanotubes and onion-like carbon. It was shown that for all investigated gases the cooling curves of the conductivity of the OLC have no anomalies and are linear in the $\ln[\sigma(T)/\sigma(300\text{K})]$ - $T^{-1/2}$ axis. On the other hand the conductivity of MWNTs during the cooling was decreased in comparison with helium in temperature interval from 200 K up to boiling point of various gases used in this work.

During the heating of the samples the decrease of conductivity both of OLC and MWNTs was observed. The main decrease of the conductivity took place in the vicinity of temperatures of the melting and condensation of environment gas. The largest changes of the conductivity were observed in the case of oxygen and methane. The weakest effect was observed for hydrogen.

The first cycle of measurements after the gas replacement results in an irreversible downturn of conductivity for helium-oxygen and helium-air atmospheres. But during next measurements the conductivity behavior becomes reversible. We have proposed that the anomalies on the heating part of conductivity curves of MWNTs and OLC at melting and vaporization temperatures of environment gas is related to capillary condensation process. This process decreases the quantity of contacts between nanotubes or onion-like carbon as described above and thus leads to a decrease in the number of current paths. In experiments with air and oxygen the conductivity is not restored after first cycle owing to irreversible destruction of contact between nanotubes or carbon onions or residual oxygen adsorption.

Presented results demonstrate a possibility of application of multiwalled carbon nanotubes for creation of stable and reversible gas sensors in the range of the melting and vaporization temperatures of investigated gases.

Acknowledgements

The work was supported by Ministry of Education and Sciences of Russian Federation (Grant N: РНП.2.1.1.1604), by the grant of the president of the Russian Federation for Scientific School (Grant N: NSh-4419.2006.3), and by the government contracts FCP № 02.513.11.3314 and № 02.513.11.3348.

References

[1] Y. X. Liang, Y. J. Chen, T. H. Wang, Appl. Phys. Lett. **85**, 666 (2004).
[2] L. Valentini, F. Mercuri, I. Armentano, C. Cantalini, S. Picozzi, L. Lozzi, S. Santucci, A. Sgamellotti, J.M. Kenny, Chem. Phys. Lett. **387**, 356 (2004).
[3] Y. L. Liu, H. F. Yang, Y. Yang, Z. M. Liu, G. L. Shen, R. Q. Yu, Thin Solid Films **497**, 355 (2006).
[4] Yu. S. Nechaev, Physics-Uspekhi **49**, 581 (2006).
[5] Y. Kojima, Y. Kawai, A. Koiwai, N. Suzuki, T. Haga, T. Hioki, K. Tange, J. Alloy. Comp. **421**, 204 (2006).
[6] P. A. Gauden, A. P. Terzyk, G. Rychlicki, P. Kowalczyk, K. Lota, E. Raymundo-Pinero, E. Frackowiak, F. Beguin, Chem. Phys. Lett. **421**, 409 (2004).
[7] E. Couteau, K. Hernadi, J. W. Seo, L. Thien-Nga, Cs. Miko, R. Gaal, L. Forro, Chem. Phys. Lett. **378**, 9 (2003).
[8] A. Magrez, J. W. Seo, V.L. Kuznetsov, L. Forro, Angewandte Chemie-International Edition. **46**, 441 (2006).
[9] V. L. Kuznetsov, Yu. V. Butenko, A. L. Chuvilin, A. I. Romanenko, A. V. Okotrub, Chem. Phys. Lett. **336**, 397 (2001).
[10] A. I. Romanenko, O. B. Anikeeva, A. V. Okotrub, L. G. Buluseva, V. L. Kuznetsov, Y. V. Butenko, A. L. Chuvilin, C. Dong, Y. Ni, Physics of the Solid State **44**, 487 (2002).
[11] A. I. Romanenko, A. V. Okotrub, V. L. Kuznetsov, A. S. Kotosonov, Physics-Uspekhi **48**, 958 (2005).
[12] N. F. Mott, E. A. Davis, Electron Processes in Noncrystalline Materrials, 2nd ed. (Oxford, Clarendon Press, 1979).
[13] A. Hunt, Solid State Comm. **86**, 765 (1993).
[14] S. V. Demishev, A. A. Pronin, V. V. Glushkov, N. E. Sluchanko, N. A. Samarin, M. V. Kondrin, A. G. Lyapin, V. V. Brazhkin, T. D. Varfolomeeva, S. V. Popova, JETP **95**, 123 (2002).
[15] A. S. Kotosonov, V. V. Atrazhev, JETP Lett. **72**, 53 (2000).
[16] A. S. Kotosonov, D. V. Shilo, Mol. Mater. **13**, 113 (2000).
[17] A. I. Romanenko, O. B. Anikeeva, A. V. Okotrub, L. G. Buluseva, N. F. Yudanov, C. Dong, Y. Ni, Physics of the Solid State **44**, 659 (2002).
[18] A. I. Romanenko, O. B. Anikeeva, T. I. Buryakov, E. N. Tkachev, A. V. Okotrub, V. L. Kuznetsov, A. N. Usoltseva, A. S. Kotosonov, NATO Science Series II: Mathematics, Physics and Chemistry **241**, 23 (2007).
[19] T. I. Buryakov, A. I. Romanenko, O. B. Anikeeva, V. L. Kuznetsov, A. N. Usol'tseva, E. N. Tkachev, JETP **105**, 155 (2007).
[20] E. N. Tkachev, A. I. Romanenkov, O. B. Anikeeva, T. I. Buryakov, V. E. Fedorov, A. S. Nazarov, V. G. Makotchenko, V. L. Kuznetsov, A. N. Usol'tseva, JETP **105**, 223 (2007).
[21] A. I. Romanenko, O. B. Anikeeva, R. V. Gorbachev, E. I. Zhmurikov, K. V. Gubin, P. V. Logachev, M. S. Avilov, S. V. Tsybulya, G. N. Kryukova, E. B. Burgina, L. Tecchio, Inorganic Materials **41**, 451 (2005).
[22] E. I. Zhmurikov, A. I. Romanenko, O. B. Anikeeva, K. V. Gubin, E. B. Burgina, S. V. Tsybulya, A. T. Titov, L. Tecchio, Inorganic Materials **42**, 609 (2006).
[23] A. I. Romanenko, O. B. Anikeeva, V. L. Kuznetsov, A. N. Obrastsov, A. P. Volkov, A. V. Garshev, Solid State Commun. 137 (2006) 625.
[24] A. S. Kotosonov, Sov. Phys. JETP **66**, 1068 (1987).
[25] A. S. Kotosonov, Carbon **26**, 735 (1988).
[26] C. V. Haesendonck, L. Stockman, R. J. M. Vullers, Y. Bruynseraede, L. Langer, V. Bayot, E. Grivei, J.-P. Issi, J. P. Heremans and C. H. Olk, Surf. Sci. **386**, 279 (1997).
[27] J. Zhao, A. Buldum, J. Han, J. Ping Lu, Nanotechnology **13**, 195 (2002).
[28] S.-H. Jhi, S. G. Louie, M. L. Cohen, Phys. Rev. Lett. **85**, 1710 (2000).
[29] V.L.Kuznetsov, A.L. Chuvilin, Yu.V.Butenko, I. Yu. Malkov, V. M. Titov, Chem.Phys.Lett., **222**, 343-348 (1994).
[30] A. Magrez, Cs. Miko, J.W. Seo, K. Hernadi, L. Forro, J. Phys. Chem. B **109/20**, 10087-10091 (2005)

*Corresponding author: air@che.nsk.su,
anatoly.roman@gmail.com